Surface Science 100 (1980) 302–314

VARIATIONS OF WORK FUNCTION AND SURFACE CONDUCTIVITY ON CLEAN CLEAVED ZINC OXIDE SURFACES BY ANNEALING AND BY HYDROGEN ADSORPTION

H. MOORMANN *, D. KOHL and G. HEILAND

2. Physikalisches Institut der Rheinisch-Westfälischen Technischen Hochschule Aachen, Templergraben 55, D-5100 Aachen, Germany

Received 11 April 1980; accepted for publication 4 June 1980

Crystals are cleaved in UHV normal and parallel to the *c* axis exposing polar and prism faces. Work function (Kelvin) and surface conductivity are measured, also after annealing at elevated temperatures in UHV and after adsorption of atomic hydrogen. The work function of all three faces decreases irreversibly by annealing in UHV, but only on the Zn face a measurable surface conductivity appears. Also hydrogen adsorption diminuishes the work function. Simultaneously an increasing surface conductivity can be observed on all three types of surfaces. Corresponding structures in the annealing curves demonstrate a correlation between work function and surface conductivity. By means of space charge calculations band bending values are derived and thereby the electron affinity, which is not accessible to direct measurement. It is concluded that the two clean cleaved polar faces exhibit a depletion layer, which remains on the O face also after annealing in UHV. On the prism face nearly flat band situation is found. The decrease of work function with increasing hydrogen coverage, i.e. surface electron density, can be interpreted by means of space charge calculations using the measured surface conductivity. For the two polar faces the band bending alone causes the decrease, whereas for the prism face an additional increase of electron affinity has to be assumed. The variation of electron affinity by annealing or by hydrogen adsorption might be due to a change of atomic distances in the uppermost layer, although no superstructure has been found in LEED studies.

1. Introduction

Surface properties of ZnO are treated in a recent review article [1]. In the hexagonal wurtzite structure three low index planes can be distinguished: The prism faces $(10\bar{1}0)$ are found on crystals as grown from the vapor phase or after cleavage parallel to the *c* axis. The zinc (0001) and oxygen $(000\bar{1})$ polar faces can be prepared by cleavage normal to the *c* axis.

The influence of annealing in ultrahigh vacuum (UHV) on electronic and chem-

* Present address: Siemens AG, WIS TE 421, Balanstrasse 73, D-8000 München, Germany.

ical properties of clean as grown prism faces has been studied in connection with the adsorption of oxygen [2]. From several arguments, e.g. isotopic exchange of oxygen at 300 K, it is concluded, that by transient heating above 700 K an increased density of point defects (donors) is produced with an inhomogeneous distribution from the surface towards the interior of the crystal.

Clean polar faces have been prepared by cleavage [3,4]: Only the Zn face exhibits an increase of surface conductivity by annealing in ultrahigh vacuum (UHV), connected with the appearance of an accumulation layer. In contrast, on the clean cleaved oxygen face remains a depletion layer also after annealing in UHV [5].

Adsorption of atomic hydrogen produces surface donors and an accumulation layer on all three low index faces [6,3]. The increase of surface conductivity proceeds much faster on the O face than on the Zn face [3].

Instabilities showing up in Hall mobility and work function of clean cleaved polar faces have been studied previously [7]. Stability criteria for the surface crystallographic structure of the polar faces have been derived [8]. They predict reconstructed surfaces. Computer calculations based on LEED observations were performed with the result that the uppermost atomic layer of the zinc and of the prism face might be shifted by a few tenth of an angstrom towards the bulk.

This reconstruction might cause changes of work function, electron affinity and band bending. In the present paper we have studied these surface properties especially in connection with surface instabilities induced by annealing in UHV and by adsorption of hydrogen.

2. Experimental

The crystals were grown from the vapor phase in the form of hexagonal prisms having a diameter of about 2 mm and a length of 15 mm. A copper doping was used to obtain a low bulk conductivity of 10^{-3} ohm^{-1} cm^{-1} at 300 K. The work function was measured by the Kelvin method. The vibrating gold electrode was driven by an electric coil with a frequency of 70 s^{-1}. For absolute values a silicon crystal serving as a reference could be cleaved several times in the same ultrahigh vacuum of 3×10^{-9} Pa (fig. 1). The work function of the freshly cleaved silicon (111) face was taken to be 4.83 eV from Allen and Gobeli [9]. Across the face the work function varied by ±0.02 eV probably due to steps. Averaged values were used. The maximum change of work function of the Kelvin electrode during the measurement of a whole hydrogen treatment curve (fig. 6) was a decrease by 0.03 eV. The work function of gold was found during all measurements within the range $4.03 < \phi_{Au} < 4.27$ eV. The cleavage of polar faces in UHV has been described previously [7]. Surface conductivities on the cleaved surfaces were measured after Van der Pauw [10] and increased by exposure to atomic hydrogen (hot filament) [6]. The tilting angles given in fig. 4 are determined using the reflection of a He–Ne laser beam.

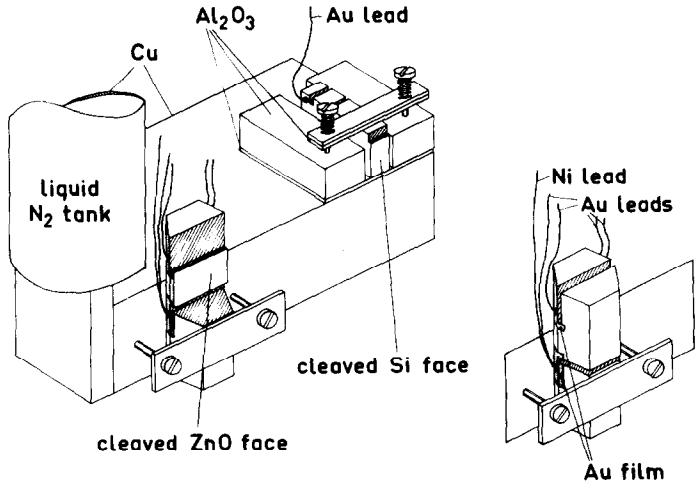

Fig. 1. Experimental arrangement. ZnO prism face and Si(111) reference, both cleaved in ultra-high vacuum.

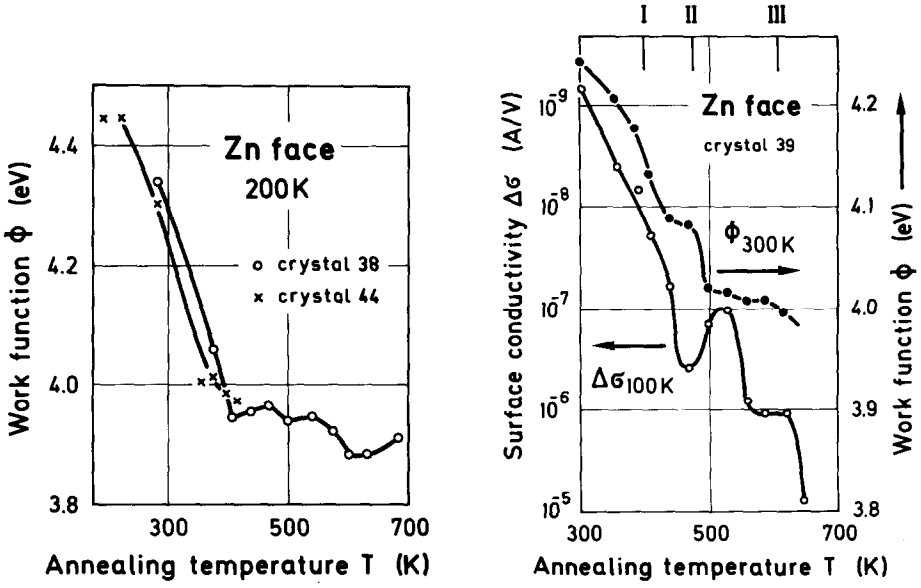

Fig. 2. Work function ϕ at 200 K as a function of the annealing temperature. Cleavage at 200 K in UHV. Both crystals were annealed 5 min for each point and measured at 200 K.

Fig. 3. Work function ϕ at 300 K and surface conductivity $\Delta\sigma$ of a Zn face at 100 K as a function of the annealing temperature. Cleavage at 300 K in UHV. The minima of $(1/\Delta\sigma)\,\delta\sigma/\delta T$ are indicated above I, II and III.

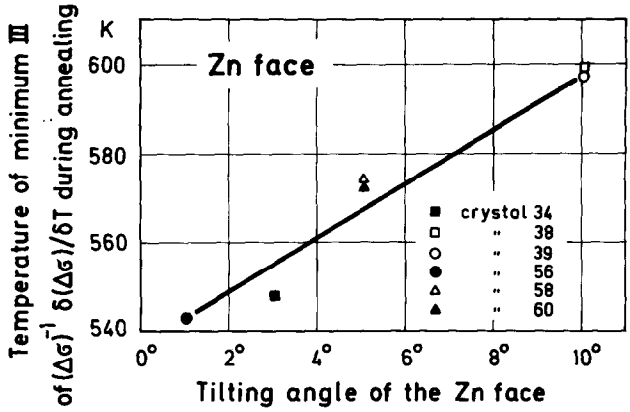

Fig. 4. Temperature of minimum III (compare fig. 3) as a function of the tilting angle between the c axis and the normal to the cleaved face.

3. Results

Figs. 2 and 3 show absolute values for the work function ϕ of Zn faces after cleavage at 200 and 300 K and after subsequent annealing. Fig. 3 contains also results about surface conductivity $\Delta\sigma$. Minimum III of $(1/\Delta\sigma)\delta\sigma/\delta T$ shifts towards higher temperatures with increasing tilting angle of the Zn face (fig. 4). Fig. 5 shows the change of work function on a cleaved prism face caused by annealing in UHV. Three crystals were investigated with similar results.

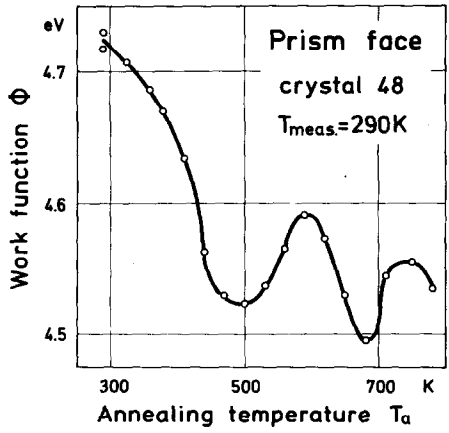

Fig. 5. Change of work function ϕ on a prism face as a function of the annealing temperature. Cleavage at 290 K.

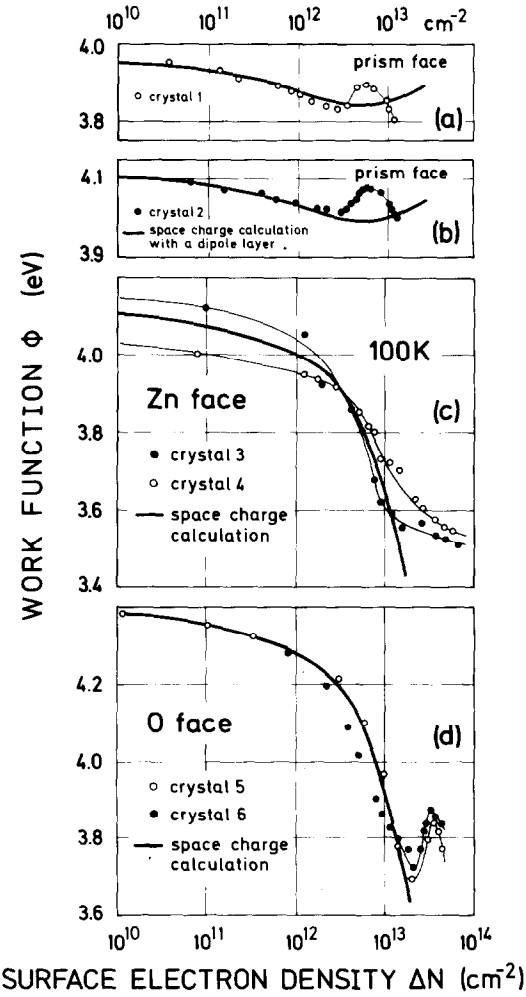

Fig. 6. Work function ϕ of cleaved polar faces as a function of surface electron density ΔN produced by hydrogen treatment. The thick line gives the result of theoretical calculations (fig. 10). (a) and (b): Cleaved prism faces of two crystals after annealing for 5 min at 500 K as a function of surface electron density ΔN; the theoretical curve includes the additional influence of one dipole per ionized donor with the negative charge on the outside (1.8 e Å). (c) and (d): Polar faces of two crystals.

The work function is also decreased by the adsorption of atomic hydrogen as can be seen in fig. 6 for the two polar faces. The surface electron density is derived from the observed surface conductivity using surface Hall effect data [11]. Corresponding studies of cleaved prism faces do not show reproducible results (4 crystals

investigated). However, after an annealing of 5 min at 500 K the results from different crystals agree as on polar faces: figs. 6a and 6b. The same holds after annealing at 570 K. But, after annealing at 620 and 670 K the work function curves of the 4 crystals are different from each other again.

4. Evaluation

Electron affinity χ and band bending qV_S can be derived from a sequence of work function and surface conductivity measurements [5]: First the work function ϕ of the freshly cleaved or annealed surface is measured at 100 K:

$$\phi_0 = \chi + (E_{CB} - E_F) - qV_{S0} .$$

Then a weak accumulation layer is established by atomic hydrogen changing work function and band bending:

$$\phi_A = \chi + (E_{CB} - E_F) - qV_{SA} .$$

The index 0 denotes the initial state of the surface, the index A the state with an accumulation layer. χ means the electron affinity, $(E_{CB} - E_F)$ the distance of con-

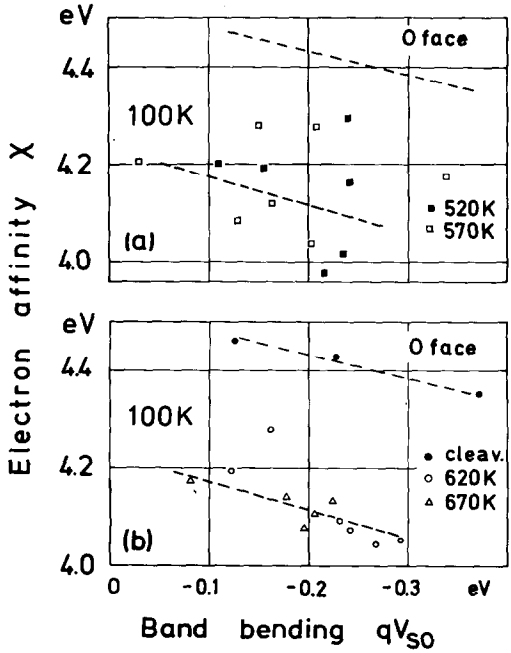

Fig. 7. Electron affinity χ of four oxygen faces as a function of band bending qV_{S0} after cleavage and after subsequent annealing. Annealing time for the indicated temperatures 300 s.

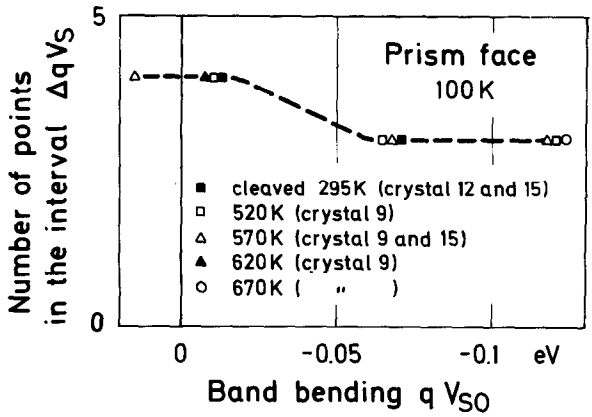

Fig. 8. Band bending qV_{S0} of freshly cleaved and of cleaved and annealed prism faces. An energy interval 0.045 eV wide is moved along the band bending scale and the number of points found in this interval is given on the vertical axis. The center of each interval is located at a measured point. The crystals were annealed for 5 min at the indicated temperature. Depletion exists for $qV_{S0} < 0$.

duction band to Fermi level in the bulk and qV_S the band bending at the surface. V_{SA} is calculated (fig. 9) from the surface carrier density (Hall effect). Using both equations χ and V_{S0} are accessible. In this analysis any influence of the hydrogen treatment on χ is neglected. Fig. 6 shows that this assumption is justified for a weak accumulation on polar surfaces. For prism faces the deviation can be calculated.

Fig. 7 gives the electron affinity of 4 oxygen faces. Whereas the values after annealing at medium temperatures show a considerable amount of scattering (fig. 7a), the values after cleavage and after annealing at higher temperature are reproducible (fig. 7b). The corresponding statistics of band bending values derived from the same experiments is given in fig. 3 of ref. [5]. An analogous plot of band bending values for the prism face can be seen in fig. 8. In both cases annealing treatments do not influence the band bending in an unique way.

5. Discussion of results on clean, cleaved and annealed surfaces

5.1. Zinc face

A change of work function by annealing of surfaces cleaved at 300 K in UHV is known for Si. Annealing at 650 K lowers the work function by 0.5 eV [12]. A similar reduction by 0.45 eV is observed on the Zn face cleaved at 200 and annealed at 360 K (fig. 2). In contrast to Si the lowering of the work function is not connected with the formation of a superstructure in the LEED pattern [4]. The onset of a measurable surface conductivity ($>10^{-10}$ A/V) is observed after anneal-

ing at 360 K (fig. 3), corresponding to a band bending of 0.13 eV [13].

At first the behaviour of the work function in the range of annealing temperature, where a measureable surface conductivity does not yet appear, shall be discussed: If the work function decrease below 360 K is attributed to a change only of band bending, then the Zn face cleaved at 200 K should exhibit a depletion layer with $qV_S = -0.3$ eV. However, a decrease of electron affinity cannot be excluded. The work function of the Zn face is reduced without the appearance of a superstructure if the distance between the uppermost zinc and oxygen layers grows. The increase can be estimated, if one neglects a change in the hybridization of involved orbitals. This neglection is probably not justified [23]. Therefore the results have to be regarded with some caution. In the following calculations the effective ionic charge is assumed to remain constant during the expansion and equal to the electronic charge. Then a change $\Delta\phi$ of -0.45 eV can be caused by an increase in layer distance of 0.24 Å during annealing up to 360 K. Above 360 K only a negligible further increase takes place. The effect is irreversible.

A layer distance differing from the bulk value was already suggested by Duke and Lubinsky [14] in order to adapt a dynamical scattering model to LEED intensity measurements of the Zn face. These authors discussed a contraction of the distance by 0.1–0.2 Å relative to the bulk value, but changes due to annealing were not considered. If the contraction process is hampered at the cleavage temperature of 230 K, an annealing treatment could lead to equilibrium positions of the atoms near the surface. However, the observed work function change has the opposite sign. Therefore an interpretation in terms of band bending is favored. That means a decrease of an initial depletion by annealing. This view is supported by the appearance of a measurable surface conductivity after annealing above 360 K (fig. 3). After cleavage at 300 K only a change of the work function by 0.04 eV appears up to 360 K. Then the upper limit for a change in the layer distance is 0.02 Å.

After annealing at temperatures below 360 K considered so far, the contributions from band bending and electron affinity to the change of work function can not be separated experimentally. For temperatures above 360 K the interpretation is simplified by the appearing of a measurable surface conductivity: fig. 3 shows that regions of steeply falling work functions are correlated with a smaller increase or even a decrease of surface conductivity. Mark I signifies not only a minimum in $(1/\Delta\sigma)\,\delta\sigma/\delta T$ but also a maximum in the first derivative of the work function. At this point the LEED contrast as a function of annealing temperature passes a minimum [4]. These facts suggest a change of crystallographic surface structure. The maximum of surface conductivity marked by II arises from a maximum of the Hall mobility [7]. The electron scattering in the space charge region can be diminuished by a higher degree of order of the surface atoms. In this case the establishment of order lowers the work function. The minimum III is connected with a steep decrease of work function at a temperature where ordered rows of steps appear in the LEED picture [4]. This temperature is a function of the tilting angle (fig. 4). Because the height of the steps is a constant equal to the hexagonal c axis [4], a

larger tilting angle means a higher density of steps. Higher densities shift the minimum III and the corresponding steep change of the work function to higher annealing temperatures. Similar to the behaviour at the temperature designated by II the appearance of a higher degree of order (regular steps) is connected with a steep change of the work function (fig. 3).

Using the mobility values of Veuhoff and Kohl [11] and the compensation model [13] the increase of band bending can be calculated from surface conductivity. Rising the annealing temperature from 360 to 600 K yields 0.2 eV. The work function is lowered by the same amount (fig. 3). That means the electron affinity is the same after annealing at 360 or 600 K. Surface Hall measurements have shown that the carrier density within the accumulation layer and also the band bending increase monotoneously from 300 to 670 K [7]. Therefore the structure of the work function curve is caused only by reversible changes of the electron affinity. If the changes of the affinity reflect the degree of order in the surface region, a connection to the results of Hall measurements appears [11].

Transitions of order might show up in LEED I/V spectra too. However, the energy carried by the electrons can change the surface structure. Photolysis happens already with UV light of 3 eV. Therefore a LEED analysis of these order transitions requires very low current densities. Such studies are not known so far.

5.2. *Oxygen face*

In contrast to the Zn face annealing temperatures between 100 and 670 K do not produce a measurable surface conductivity on the oxygen face. However, using a special cycle of measurements the contributions of band bending and electron affinity can be separated (section 4) [5]. The depletion layer with a derived band bending of about −0.2 eV remains up to annealing temperatures of at least 670 K. The electron affinity is reduced by 0.3 eV after annealing to 620 and 670 K (fig. 7b). At lower annealing temperatures huge statistical fluctuations in the electron affinity appear (fig. 7a). The decrease of the electron affinity corresponds to a decrease of the layer distance by 0.17 Å. Up to now a model linking changes of electron affinity with changes of band bending is not known. However, in order to vary the band bending it is necessary to change the energy distribution of surface state density. This distribution can be connected with surface structure [12] as well as the electron affinity. In this way the observed decrease of the electron affinity may be correlated with increasing band bending (fig. 7b).

5.3. *Prism face*

As on the oxygen face a measurable surface conductivity does not appear after annealing up to 770 K. Therefore the same cycle was used to determine the band bending (section 4) [5]. Immediately after cleavage as well as after annealing at temperatures up to 670 K the band bending is found in the interval from −0.12

to +0.02 eV (fig. 8). The observation of both signs requires the assumption of at least one acceptor and one donor surface level. A depletion of –0.12 eV can be reached by an acceptor density of at least 1×10^{11} cm^{-2} [13]. For a weak accumulation of 0.02 eV a donor density of at least 3×10^{10} cm^{-2} is needed. The narrow range of band bending after cleavage and annealing (fig. 8) allows an interpretation of the work function curve in fig. 5: The initial decrease by 0.2 eV has to be attributed to a decrease of electron affinity. The amplitude of the oscillations corresponds to the range of band bending in fig. 8.

Duke et al. [15–17] suggested a reconstructed model of the prism face. This model is further supported by photoemission studies [18]. The oxygen atoms should be shifted inwards by 0.05 Å and the zinc atoms by 0.45 Å. This models leads to a decrease of the electron affinity by 1.08 eV compared to the unrelaxed surface. As can be seen from fig. 5 the work function decreases already after the first annealing at 320 K after cleavage. It is possible that the surface cleaved at room temperature has not yet reached an equilibrium state. Only by annealing at 470 K a stable final state can be reached which might correspond to the state proposed by Duke et al. A similar stabilization by annealing after cleavage was described in section 3 for hydrogen adsorption. Reproducible results could only be obtained, if the crystals were preannealed at 500 or 570 K. This transition to an equilibrium state does not influence the surface states causing the band bending (fig. 8).

6. Discussion of results on adsorption of atomic hydrogen

The treatment with atomic hydrogen increases the carrier density in the space charge layer by several orders of magnitude on the polar faces as well as on the prism face (fig. 6). The band bending contributing to the measured work function can be derived from model calculations of the space charge layer. Some results of these calculations are shown in figs. 9 and 10.

For weak accumulation layers the bulk traps must be considered in detail. This part of the curve is denoted by "Compensation model" [13]. Beginning degeneracy with electron densities above 5×10^{10} cm^{-2} removes the temperature dependence of the density [11]. A simple model for higher carrier densities is based on the assumption of a triangle potential well neglecting the influence of the static charge in bulk defects [19]. However, the bulk of ZnO is highly compensated with point defect densities of about 10^{16} cm^{-3} [20]. Therefore the triangle potential is not considered. A parabolic potential arises from the assumption of a homogeneously distributed static charge of concentration ρ. The energy levels (lower edges of the subbands) are given by

$$E_n = (e\rho hn/8m\epsilon\epsilon_0)^{1/2}\,, \qquad n = 1, 2, \ldots .$$

The connection between band bending and carrier concentration was calculated in

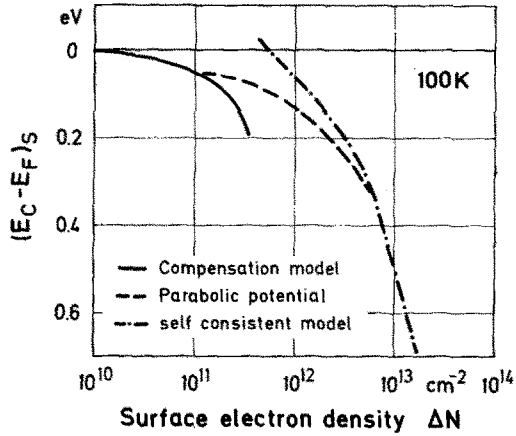

Fig. 9. Distance between conduction band edge and Fermi level at the surface $(E_C - E_F)_S$ as a function of surface electron density ΔN. Results of three different model calculations. Since the range of validity is limited for each model, one has to interpolate to cover the whole density range. The resulting curve is given in figs. 6c and 6d.

the same way as for the triangular potential. The influence of trapped charge in the bulk disappears for electron densities above 10^{13} cm^{-2}. A self consistent calculation neglecting bulk traps allows a description of the space charge layer [21]. In this regime the calculation of the band bending is supported by results of capacitance measurements in an electrolyte [21].

Paying attention to the regions of validity of the model calculations, the comparison of measured and theoretical curves in figs. 6c and 6d shows that the

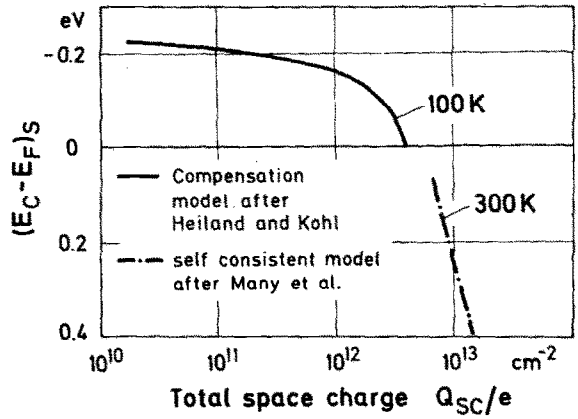

Fig. 10. Results of two model calculations for the total space charge as used for the dipole contribution in figs. 6a and 6b.

decrease of the work function on the polar faces can be explained by a variation of the band bending alone up to densities of 10^{13} cm^{-2}.

Apparently the electron affinity is not changed by the adsorption of hydrogen. Therefore only adsorption sites are allowed where the dipole moment of the hydrogen bond at the surface disappears. The hydrogen might be located in the plane of the uppermost atomic layer on the polar faces, perhaps in a sort of bridge bonding between neighbouring zinc and oxygen atoms.

On the prism face (figs. 6a and 6b) the theoretical curve of the band bending calculations decays steeper than the curve of the measured work function values. At a density of 10^{13} cm^{-2} the deviation between measured and calculated values amounts to 0.3 eV. In this case the electron affinity should increase. The picture of a negatively charged hydrogen atom above the uppermost layer of an ideal prism face seems not probable. If the uppermost layer contains the hydrogen ions a shift of the oxygen and zinc atoms of this layer would be possible. This shift might enlarge the electron affinity (fig. 6) if the oxygen atoms move outwards or the zinc atoms inwards.

The discussed nonperiodic disorder of the uppermost lattice plane should lead to a lower electron mobility in the space charge layer [11]. The measured values of the Hall mobility at 100 K reach at maximum about 100 $cm^2/V \cdot s$ on the prism face but coincide with the bulk value of about 1000 $cm^2/V \cdot s$ on both polar faces [11]. Above an electron density of 10^{13} cm^{-2}, prism and polar faces show structures in the work function which are characteristic for the type of the face (fig. 6) and which are not explained by the space charge calculations. The deviations must be caused by pecularities of the electron affinity.

Note added in proof

In figs. 9 and 10 the numbers on the ordinate should be taken with the opposite sign.

Acknowledgement

The work was supported by the Deutsche Forschungsgemeinschaft via the Sonderforschungsbereich "Festkörperelektronik" at Aachen.

References

[1] G. Heiland and H. Lüth, Adsorption on Oxides, in: Chemical Physics of Solid Surfaces and Heterogeneous Catalysis, Vol. III, Chemisorption Systems, Ed. D.A. King (Elsevier, Amsterdam, in press).

[2] W. Göpel, J. Vacuum Sci. Technol. 15 (1978) 1298.
[3] G. Heiland and P. Kunstmann, Surface Sci. 13 (1969) 72.
[4] D. Kohl, M. Henzler and G. Heiland, Surface Sci. 41 (1974) 403.
[5] H. Moormann, D. Kohl and G. Heiland, Surface Sci. 80 (1979) 261.
[6] G. Heiland, Z. Physik 148 (1957) 15.
[7] D. Kohl and G. Heiland, Surface Sci. 63 (1977) 96.
[8] R.W. Nosker, P. Mark and J.D. Levine, Surface Sci. 19 (1970) 291.
[9] F.G. Allen and G.W. Gobeli, Phys. Rev. 127 (1962) 150.
[10] L.J. van der Pauw, Philips Res. Rept. 13 (1958) 1.
[11] E. Veuhoff and D. Kohl, in preparation.
[12] W. Mönch, Festkörperprobleme 13 (1973) 241.
[13] G. Heiland and D. Kohl, Phys. Status Solidi (a) 49 (1978) 27.
[14] C.B. Duke and A.R. Lubinsky, Surface Sci. 50 (1975) 605.
[15] C.B. Duke, A.R. Lubinsky, S.C. Chang, B.W. Lee and P. Mark, Phys. Rev. B15 (1977) 4865.
[16] C.B. Duke, A.R. Lubinsky, B.W. Lee and P. Mark, J. Vacuum Sci. Technol. 13 (1976) 761.
[17] C.B. Duke, R.J. Meyer, A. Paton and P. Mark, Phys. Rev. B18 (1978) 4225.
[18] W. Göpel, R.S. Bauer and G. Hansson, in press.
[19] G. Dorda, Festkörperprobleme 13 (1973) 215.
[20] S. Trokman, A. Many, Y. Goldstein, G. Heiland, D. Kohl and H. Moormann, J. Phys. Chem. Solids, to be published.
[21] D. Eger, A. Many and Y. Goldstein, Phys. Letters 55A (1975) 197.
[22] R.P. Eischens, W.A. Pliskin and M. Low, J. Catalysis 1 (1962) 180.
[23] W.A. Goddard III, J.J. Barton, A. Redondo and T.C. McGill, J. Vacuum Sci. Technol. 15 (1978) 1274.